

Dynamic volumetric changes of hippocampal subfields in clinically isolated syndrome patients: A 2-year MRI study

Laura Cacciaguerra, Elisabetta Pagani, Sharlota Mesaros, Jelena Dackovic, Irena Dujmovic-Basuroski, Jelena Drulovic, Paola Valsasina, Massimo Filippi  and Maria Assunta Rocca 

Abstract

Background: Different subregional patterns of hippocampal involvement have been observed in diverse multiple sclerosis (MS) phenotypes.

Objective: To evaluate the occurrence of regional hippocampal variations in clinically isolated syndrome (CIS) patients, their relationships with focal white matter (WM) lesions, and their prognostic implications.

Methods: Brain dual-echo and three-dimensional (3D) T1-weighted scans were acquired from 14 healthy controls and 36 CIS patients within 2 months from clinical onset and after 3, 12, and 24 months. Radial distance distribution was assessed using 3D parametric surface mesh models. A cognitive screening was also performed.

Results: Patients showed clusters of reduced radial distance in the Cornu Ammonis 1 from month 3, progressively extending to the subiculum, negatively correlated with ipsilateral T2 and T1 lesion volume. Increased radial distance appeared in the right dentate gyrus after 3 ($p < 0.05$), 12, and 24 ($p < 0.001$) months, and in the left one after 3 and 24 months ($p < 0.001$), positively correlated with lesional measures. Hippocampal volume variations were more pronounced in patients converting to MS after 24 months and did not correlate with cognitive performance.

Conclusion: Regional hippocampal changes occur in CIS, are more pronounced in patients converting to MS, and are modulated by focal WM lesions.

Keywords: Shape analysis, longitudinal analysis, hippocampus, dentate gyrus, multiple sclerosis, MRI

Date received: 8 January 2018; revised: 6 June 2018; accepted: 14 June 2018

Introduction

Multiple sclerosis (MS) is the most common demyelinating disease of the central nervous system (CNS) of young adults. MS pathology includes inflammation and neurodegeneration, affecting both the white matter (WM) and gray matter (GM). Widespread GM involvement was described from the initial stages of the disease by magnetic resonance imaging (MRI)¹ and pathological² studies.

The hippocampus is a GM area affected in MS and its involvement is clinically relevant, being associated with visuospatial and mnemonic deficits.^{3–5} Histological studies have demonstrated diffuse demyelination, plaque formation, and axonal loss in the hippocampus

of MS patients.^{6,7} Using MRI, hippocampal lesions⁸ and atrophy^{4,5} have been found. Anatomically, the hippocampus is a small-sized structure of archicortex consisting of two laminae, separated by the hippocampal sulcus: the Cornu Ammonis (CA), composed by four subfields (CA1, CA2, CA3, CA4), and the dentate gyrus (DG). A transitional cortex, called subiculum, divides the CA from the rest of the temporal lobe. CA subregions show different susceptibility to damage, with the CA1 region known to be the most involved in many neurological conditions (e.g. temporal epilepsy, Alzheimer's disease, and ischemia),^{9–11} whereas the CA2 is the most preserved one.⁹ In MS, hippocampal demyelination mirrors such a pattern of

Multiple Sclerosis Journal

2019, Vol. 25(9) 1232–1242

DOI: 10.1177/

1352458518787347

© The Author(s), 2018.

Article reuse guidelines:
sagepub.com/journals-
permissions

Correspondence to:

MA Rocca

Neuroimaging Research Unit,
Institute of Experimental
Neurology, Division
of Neuroscience, San
Raffaele Scientific Institute,
Vita-Salute San Raffaele
University, Via Olgettina 60,
20132 Milan, Italy.
rocca.mara@hsr.it

Laura Cacciaguerra

Massimo Filippi

Maria Assunta Rocca

Neuroimaging Research Unit,
Institute of Experimental
Neurology, Division
of Neuroscience, San
Raffaele Scientific Institute,
Vita-Salute San Raffaele
University, Milan, Italy/
Department of Neurology,
Institute of Experimental
Neurology, Division
of Neuroscience, San
Raffaele Scientific Institute,
Vita-Salute San Raffaele
University, Milan, Italy

Elisabetta Pagani

Paola Valsasina

Neuroimaging Research Unit,
Institute of Experimental
Neurology, Division
of Neuroscience, San
Raffaele Scientific Institute,
Vita-Salute San Raffaele
University, Milan, Italy

Sharlota Mesaros

Jelena Dackovic

Irena Dujmovic-Basuroski

Jelena Drulovic

Clinic of Neurology, Faculty
of Medicine, University of
Belgrade, Belgrade, Serbia

vulnerability, with most lesions occurring in the CA1 and sparing the CA2.⁶ MRI studies described a gradient of progressive hippocampal involvement among the main MS clinical phenotypes, with a selective atrophy of the CA1 in relapsing–remitting patients, whereas in those with secondary progressive MS, other regions are also affected.⁴

Besides these pieces of evidence of regional atrophy, another, small, subfield of the hippocampus, the DG, is known to be a site of adult neurogenesis, which occurs into its subgranular layer every day.¹² This phenomenon is thought to play a central role in hippocampal-dependent memory,¹³ long-term potentiation,¹⁴ and synaptic plasticity.¹⁵ Using MR-based radial mapping analysis, an expansion of the DG was recently detected in relapse-onset MS patients, which was more pronounced in the inflammatory phase of the disease and was associated with better cognitive performance (at that stage).¹⁶

There remain, however, several unexplored aspects of hippocampal involvement in MS, including the time of onset and evolution of hippocampal subregional abnormalities, the influence of inflammatory activity, and their possible prognostic implications. To answer these questions, the ideal target population should have a supposed recent biological disease onset, have suffered a fresh inflammatory event, and be treatment-free (to avoid possible confounding effects of disease-modifying drugs). We performed a 2-year longitudinal study in which we analyzed hippocampal shape using surface-based mesh modeling¹⁷ in subjects with clinically isolated syndrome (CIS), their correlations with WM lesion volume (LV) and cognitive performance, and their role for the development of MS.

Materials and methods

Ethics committee approval

Approval was received from local ethical standards committee on human experimentation, and written informed consent was obtained from all subjects.

Subjects

We enrolled a consecutive cohort of 37 CIS patients and 14 age- and sex-matched healthy controls (HCs), studied in a previous work,¹⁸ who underwent a brain MRI acquisition, a neurological evaluation (comprehensive of Expanded Disability Status Scale (EDSS) assessment), and a neuropsychological screening at baseline (within 2 months from clinical onset) and after 3 (M3), 12 (M12), and 24 (M24) months. At baseline, cerebrospinal fluid

(CSF) examination was also obtained from all patients. In our prior work, a voxel-wise analysis of brain GM and WM volume changes and WM microstructural damage in CIS patients was performed.¹⁸

Subjects with previous history of neurological/psychiatric illness, substances abuse, and steroid administration during the month before study enrollment were excluded.

Within 48 hours of the MRI, an expert neuropsychologist administered the Paced Auditory Serial Addition Test (PASAT3) extracted from the Multiple Sclerosis Functional Composite (MSFC) battery, to assess attention, working memory, and information processing speed functions. A test score more than 1.5 standard deviations (SDs) below the normative value of Serbian population¹⁹ was considered abnormal. Variation of cognitive function on the test was assessed by calculating a reliable change index (RCI) with correction for measurement error and practice effects.²⁰ RCI scores <-1.25 were related to worsening.

MRI acquisition and analysis

Using a 1.5 Tesla system (Avanto, Siemens Medical, Erlangen, Germany) under a program of regular maintenance, the following brain images were acquired from all subjects: (1) axial dual-echo turbo spin-echo (repetition time (TR)=2650 ms, echo time (TE)=28–113 ms, echo train length (ETL)=5, number of slices=50, slice thickness=2.5 mm with no gap, matrix size=256×256, field of view (FOV)=250×250 mm²), (2) sagittal three-dimensional (3D) T1-weighted magnetization prepared rapid acquisition gradient echo (MPRAGE) (TR=2000 ms, TE=3.93 ms, inversion time=1100 ms, number of sections=208, section thickness=0.9 mm, matrix size=256×224, FOV=236×270 mm²), and (3) post-contrast (0.1 mmol/kg of gadolinium (Gd) DTPA; acquisition delay: 5 minutes) sagittal 3D T1-weighted MPRAGE (using the same parameters as the pre-contrast sequence).

All scans were positioned at baseline and follow-up following standardized guidelines.

T2-hyperintense, T1-hypointense, and Gd-enhancing lesions were identified by consensus of two experienced observers blinded to the patients' identity, and global and hemispheric LVs were measured (Jim 6.0, <http://www.xinapse.com>, Xinapse Systems, Colchester, UK; see Supplementary Material). From lesion classification and count, the fulfillment of the criteria for disease dissemination in space (DIS) and disease dissemination in time (DIT) was assessed.²¹ After

T1-hypointense lesion refilling, normalized brain volumes (NBVs) and longitudinal percentage brain volume changes (PBVCs) were assessed (SIENAX and SIENA software, University of Oxford, Oxford, UK).

Hippocampal segmentation

Hippocampal segmentation was obtained from the 3D T1-weighted images.^{5,18} Correction of intensity non-uniformity was performed, and images were aligned to the Montreal Neurological Institute (MNI) space using the vtk-CISG tool and an affine transformation,²² without applying any skull stripping or masking operation, and finally reformatted into the coronal plane.¹⁷ After transformation, the original voxel size = $1 \times 1 \times 1 \text{ mm}^3$ was maintained.

One patient was excluded because of poor quality of images. An experienced observer performed manual tracing of the hippocampus, according to a standardized protocol.²³ Intra-observer reproducibility of hippocampal segmentation (evaluation of 20 randomly selected subjects twice, 2 weeks apart by one observer, and calculation of intraclass correlation coefficient) showed an intraclass correlation coefficient of 0.91. The volume of the traced structures was computed from contours by using the LONI software (MultiTracer software, Laboratory of Neuro Imaging (LONI), University of Southern California, Los Angeles, CA, USA).

To confirm the results of the manual segmentation, we performed a pilot analysis of initial timepoints using the automatic hippocampal subfield segmentation optimized for longitudinal analysis included in the FreeSurfer 6.0 software suite (Athinoula A. Martinos Center for Biomedical Imaging, Massachusetts General Hospital, Charlestown, MA, USA).²⁴

Surface-based mesh modeling

Hippocampal traces were converted to parametric surface meshes with the tool available within the library LONI Shape Tools (<http://www.loni.usc.edu/Software/ShapeTools>, version 1.3.11, Athinoula A. Martinos Center for Biomedical Imaging, Massachusetts General Hospital, Charlestown, MA, USA) and were resampled in a common number of 100×150 surface vertices, made spatially uniform and homologous with each other. From the parametric surface model of each individual hippocampus, a medial curve was derived along the antero-posterior axis, and the distance of each vertex from its medial core was calculated (radial distance (RD)). The medial core represents an intrinsic frame of reference itself, making the RD measures independent from the head positioning of the single subject.

Statistical analysis

Shapiro–Wilk test was performed to assess normality. Variables following a Gaussian distribution (i.e. age, disease duration, global hippocampal volumes) were compared between groups using two-sample *t* tests and longitudinally within groups with paired *t* test. Variables not following Gaussian distribution (i.e. EDSS, T2 LV, T1 LV, Gd LV) were compared between groups using the Mann–Whitney test and longitudinally with Wilcoxon’s test for paired data. Between-group comparison of categorical variables used Pearson χ^2 . Between-group comparisons were adjusted for age (SPSS version 21.0, IBM Corp., Armonk, NY, USA).

The intragroup longitudinal hippocampal radial mapping analysis was performed for each homologous surface vertex in CIS patients and HC with a paired *t* test in MATLAB 12. Mean changes in RD between timepoints were also calculated and plotted on HC average hippocampal surface. Non-parametric Spearman correlation, controlling for age, was run at each surface point to map correlation between RD and T2-, T1-, and Gd ipsilateral hemispheric LV at each timepoint and their changes between timepoints.

Radial mapping analysis and correlations were corrected for multiple comparisons using false discovery rate (FDR).

A surface map of different hippocampal subfields (CA1-4, DG, and subiculum) based on anatomical data was overlapped on the average hippocampal shape of each group,⁵ to standardize the anatomical location of significant modifications in RD.

All previous analyses were repeated considering CIS patients according to their evolution or not to MS (second clinical attack) during the follow-up.

Results

Clinical and conventional MRI data

CIS patients (29/7 women/men; mean age = 30.5 years, SD = 6.8) and HC (10/4 women/men; mean age = 33.6 years, SD = 7.9) did not differ for demographic features. Median disease duration in CIS was 22.6 days (range: 2–60). Table 1 summarizes the main neurological and MRI measures from HC and CIS patients. At baseline, 27 of 36 patients (75%) showed DIS, and 6 patients (17%) had both DIS and DIT. Mean baseline PASAT3 performance was 40.0 (SD = 9.9). Four patients started a disease-modifying therapy during the follow-up.

At M24, 21 of 36 (58%) had suffered a second clinical event (converter CIS (c-CIS)) and 32 (89%) had DIS and DIT according to MRI. Mean PASAT3 score was 45 (SD=8.7).

At baseline, compared to non-converters (nc), c-CIS did not differ for sex distribution (male/female=6/15 vs. 1/14, $p=0.2$), age, EDSS, disease duration, CSF oligoclonal bands, T2-, T1-, Gd LV, and NBV.

Longitudinal modifications of clinical and conventional MRI measures in CIS patients are summarized in Table 1 and have been previously reported.¹⁸ A significant reduction of median EDSS at M3 emerged in CIS patients ($p<0.001$), because six patients partially recovered after the first clinical event. Median RCI was 0.03 (SD=1.0), and five (13.5%) CIS patients showed a worsening at PASAT3.

Global hippocampal volume analysis

Baseline hippocampal volume did not differ between HC and CIS patients (Table 1). During the follow-up, hippocampal volume remained stable in HC. CIS patients experienced a significant increase of the left hippocampal volume at M3, which disappeared at M12. At M24, CIS patients developed significant hippocampal atrophy, bilaterally. Global hippocampal volume did not differ between c-CIS and nc-CIS at baseline (mean right 3.67 (SD=0.3) vs. 3.62 (SD=0.4) mL, $p=0.7$; left 3.58 (SD=0.3) vs. 3.52 (SD=0.3) mL, $p=0.6$) and during the follow-up (data not shown).

Radial mapping analysis

Hippocampal RD remained substantially stable during the follow-up in HC (Supplementary Figure), while CIS patients had dynamic modifications of RD. Figure 1 shows mean RD variations between timepoints in CIS patients. The right hippocampus showed a progressive enlargement of RD at M3 versus baseline ($p<0.05$), M12 versus M3 ($p<0.001$), and M24 versus baseline ($p<0.001$) in the DG subfield. Such a phenomenon was evident in the left hippocampus at M3 versus baseline, M24 versus M12, and M24 versus baseline (Figure 2). Some areas of the hippocampal head (CA1) seemed enlarged at M3 in the right hippocampus. However, this was not statistically significant at the longitudinal analysis. FreeSurfer segmentation confirmed the enlargement of the right DG and CA1 at M3 versus baseline (baseline volume of the granular cells of the molecular layer of the DG (GC-ML-DG)=0.314 vs. M3 volume=0.319 mL, $p=0.002$; baseline CA1 volume=0.626 vs. M3

volume=0.633 mL, $p=0.009$; see Supplementary Results and Table). Significant regions of reduced RD appeared in CIS patients in CA1 bilaterally at M3 ($p=0.05$ – 0.0001) and progressively enlarged at subsequent timepoints, while reduced RD of the subiculum was evident from M12, bilaterally ($p<0.001$) (Figure 2).

Similarly, both c-CIS and nc-CIS showed a progressive reduction of the RD in CA1 and subiculum bilaterally (apparently more pronounced in c-CIS), but only c-CIS developed right DG hypertrophy at M12 versus M3 ($p<0.001$; Figure 3).

Analysis of correlations

In CIS patients, T2 LV was correlated with hippocampal RD reduction, bilaterally, in the subiculum at baseline (p range: 0.05–0.01 right, 0.05–0.001 left) and at M3 (p range: 0.05–0.01 right, 0.05–0.001 left), and in the CA1 subfield of the tail at M12 and M24 (p range: 0.05–0.01 right, 0.05–0.01 left) (r values, corresponding to significant p , are shown in Figure 4). Similar results, with different p and r values, were found for T1 LV (Figure 4).

T2 LV was positively correlated with DG enlargement of hippocampus at baseline (p range: 0.01–0.001 right, 0.05–0.01 left) and M3 (p range: 0.01–0.001 right, 0.05–0.01 left). T1 LV was positively correlated with bilateral DG enlargement at baseline and M3 (p range: 0.01–0.001). Considering Gd LV and RD (Figure 4), a positive correlation between left DG RD and Gd LV was found at baseline and M24. No correlation was found between longitudinal changes of LV and RD.

No correlations were found between hippocampal RD measures and EDSS and PASAT scores.

Discussion

We estimated global and regional hippocampal volumetric changes in CIS patients during a 2-year follow-up. Our data suggest that global hippocampal volume is not affected at disease onset, but its atrophy occurs relatively early, at the end of our follow-up. A significant increase of global left hippocampal volume was detected at M3, which is in line with previous evidence of increased left temporal pole volume in CIS patients.¹⁸ Surface-based analysis showed that subregional hippocampal volume changes occur in CIS, with a coexistence of atrophy in damage-sensitive regions and hypertrophy in the DG; they seem to be influenced by local WM pathology and may have prognostic implications.

Table 1. Main neurological and conventional MRI data of HCs and CIS patients at baseline and during the follow-up.

	Baseline		M3		M12		M24		p
	HCs	CIS	HCs	p	HCs	p	HCs	p	
		p (3-0)		p (3-0)		p (12-3)		p (24-12)	
Median EDSS (range)	-	2.0 (0.0-6.0)	-	<0.001 ^a	1.5 (0.0-4.0)	ns ^a	-	1.5 (0.0-4.0)	ns ^a
Median T2 LV (range) (mL)	-	2.4 (0.0-22.5)	-	0.32 ^a	3.1 (0.1-24.7)	0.46 ^a	-	3.2 (0.1-24.7)	0.04 ^a
Median T1 LV (range) (mL)	-	0.63 (0.0-7.5)	-	0.89 ^a	0.42 (0.2-7.2)	0.36 ^a	-	0.54 (0.1-9.8)	0.80 ^a
Median Gd LV (range) (mL)	-	0.00 (0.0-0.2)	-	0.17 ^a	0.00 (0.0-0.8)	0.47 ^a	-	0.00 (0.0-0.4)	0.48 ^a
Mean baseline (SD) NBV (mL)	1561 (85)	1552 (96)	0.99 ^c	-	-	-	-	-	-
PBVC (%) in follow-up	-	-	-0.07 (0.3)	0.8 ^b	-0.13 (0.4)	0.3 ^b	-0.37 (0.61)	-0.86 (1.26)	0.1 ^b
Mean (SD) R normalized HV (mL)	3.71 (0.4)	3.64 (0.4)	0.56 ^c	0.81 ^b	3.65 (0.3)	0.99 ^b	3.68 (0.4)	3.51 (0.3)	0.99 ^b
Mean (SD) L normalized HV (mL)	3.62 (0.4)	3.55 (0.4)	0.67 ^c	0.01 ^b	3.67 (0.4)	0.87 ^b	3.67 (0.4)	3.33 (0.3)	0.11 ^b

MRI: magnetic resonance imaging; HCs: healthy controls; CIS: clinically isolated syndrome; EDSS: Expanded Disability Status Scale; LV: lesion volume; Gd: gadolinium; SD: standard deviation; NBV: normalized brain volume; PBVC: percentage brain volume change; HV: hippocampal volume; R: right; L: left; M3: 3-month follow-up; M12: 12-month follow-up; M24: 24-month follow-up. p refers to cross-sectional intergroup analysis (CIS vs. HC) at corresponding timepoints, while p(3-0), p(12-3), p(24-12), and p(24-0) refer to the paired intragroup analysis in CIS and HC at corresponding timepoints. Bold indicates significant values.
^aWilcoxon test for paired data.
^bt test for paired data.
^ct test.

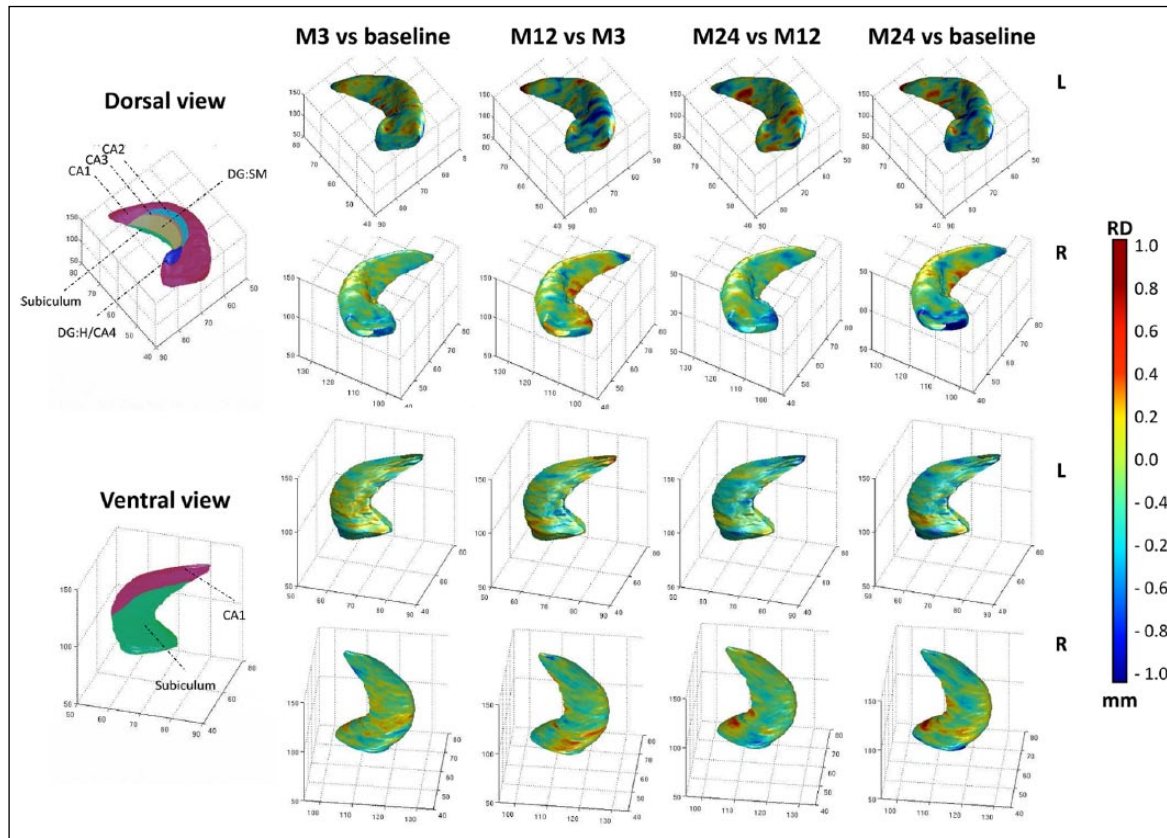


Figure 1. Schematic representation of hippocampal subfields (left side). Hippocampal mean RD longitudinal modifications in clinically isolated syndrome (CIS) patients (right side). RD values are shown in the color bar (mm). CA1: Cornu Ammonis 1 subfield; CA2: Cornu Ammonis 2 subfield; CA3: Cornu Ammonis 3 subfield; DG:SM: stratum moleculare of the DG; DG:H/CA4: hilus of the DG, that is, Cornu Ammonis 4 subfield; M3: 3 months; M12: 12 months; M24: 24 months; R: right; L: left; RD: radial distance; DG: dentate gyrus.

Despite the preserved global structure, subregional hippocampal involvement occurs from the beginning of the disease in CIS patients: bilaterally in the CA1 region, progressively spreading to the head, following the CA1 profile, and along the subiculum.

These findings confirm the higher susceptibility to damage of CA1 and subiculum subfields previously described, which seems independent from the etiology of the pathological noxa.^{4,25} Considering demyelinating-inflammatory conditions like MS, pathological and MRI studies have shown prevalent CA1 damage in the inflammatory phase of the disease, while other subfields became affected only during the progressive course.⁴

To define the influence of focal WM lesions on hippocampal volume modifications, we performed an analysis of correlation which showed a negative relationship between reduction of CA1 and subiculum RD and ipsilateral hemispheric T2 and T1 LV, while

Gd LV was scarcely correlated. These data suggest that regional hippocampal atrophy development parallels sustained focal WM damage and is marginally influenced by transient acute inflammatory activity.

The regional subfield analysis allowed us also to detect a transient increase of RD in the DG subfield, which was asynchronous between the two hemispheres. Such a lateralization cannot be explained by any difference of LV, as LVs of the two hemispheres did not differ at any timepoint (data not shown).

Several mechanisms can contribute to explain enlargement of the DG in CIS patients and its longitudinal modifications. The DG is a site of adult neurogenesis, which is regulated by many different stimuli. It is reduced in neurodegenerative diseases^{26,27} but also after acute inflammation.²⁸ Neurogenesis is a complex process, evolving over different stages: neuronal progenitor cell (NPC) proliferation in the subgranular zone of the DG, migration of newborn

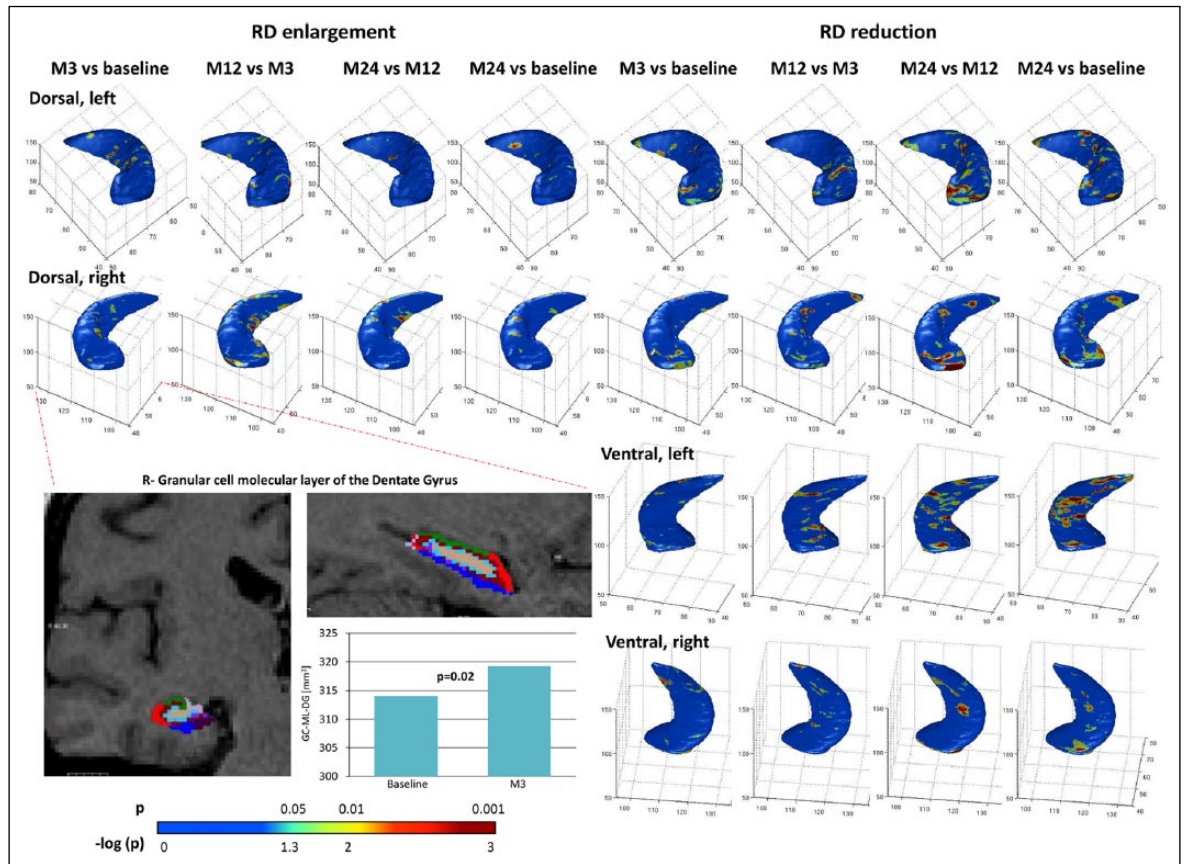


Figure 2. Longitudinal variations of radial distance (RD) in clinically isolated syndrome patients. Left side: Surface distribution of regions of significant local enlargement detected with manual segmentation (up) and with automatic FreeSurfer 6.0 segmentation after 3 months (down). Right side: Surface distribution of regions of significant local atrophy detected with manual segmentation; p value ranges in the color bar are reported as $-\log(p)$ value. M3: 3 months; M12: 12 months; M24: 24 months; GC-ML-DG: granule cell layer of the dentate gyrus.

neuroblasts into the granular layer, and finally differentiation into mature neurons/astrocytes.²⁹ Impaired neurogenesis occurs when any of these steps are affected. A recent study demonstrated that while an inflammatory environment initially promotes hippocampal NPC proliferation, it also reduces the capacity of these cells to generate mature neurons and, over the long term, modifies NPC differentiation, by shifting their fate toward the glial cell lineage.³⁰ During neurogenesis, surveillant microglia are suggested to regulate the fate and development of adult-born neurons.³¹ In line with this, using MR-based radial mapping, an increased RD in DG of MS patients has been found.¹⁶ Based on these data, it is tempting to speculate that increased DG RD could be a physiological compensatory response of neurogenesis during the initial stages of the disease, and, in later stages, could be only the epiphenomenon of gliogenesis. That microglia activation might play a role in explaining our findings is supported by a recent positron emission tomography study in CIS patients, which showed

an increase of microglia activation in these patients.³² In the absence of pathological assessment, we cannot rule out that factors different from an increased neuron formation may contribute to explain increased DG RD, including an increased turnover of non-neuronal cells (vascular cells, etc.),¹² increased dendritic complexity of existing mature cells, or increased amount of extracellular fluid.

Another point of interest is whether burden of inflammation could influence hippocampal neurogenesis.³³ Our data showed a positive correlation between DG expansion and lesional measures, in line with previous findings that evidenced a positive correlation between the number of proliferating progenitors in the DG and the degree of brain inflammation.³⁴

Since the hippocampus is involved in cognitive functions, we explored the correlation between hippocampal volumetric modifications and PASAT, which was used as a screening measure of cognitive failure. Not

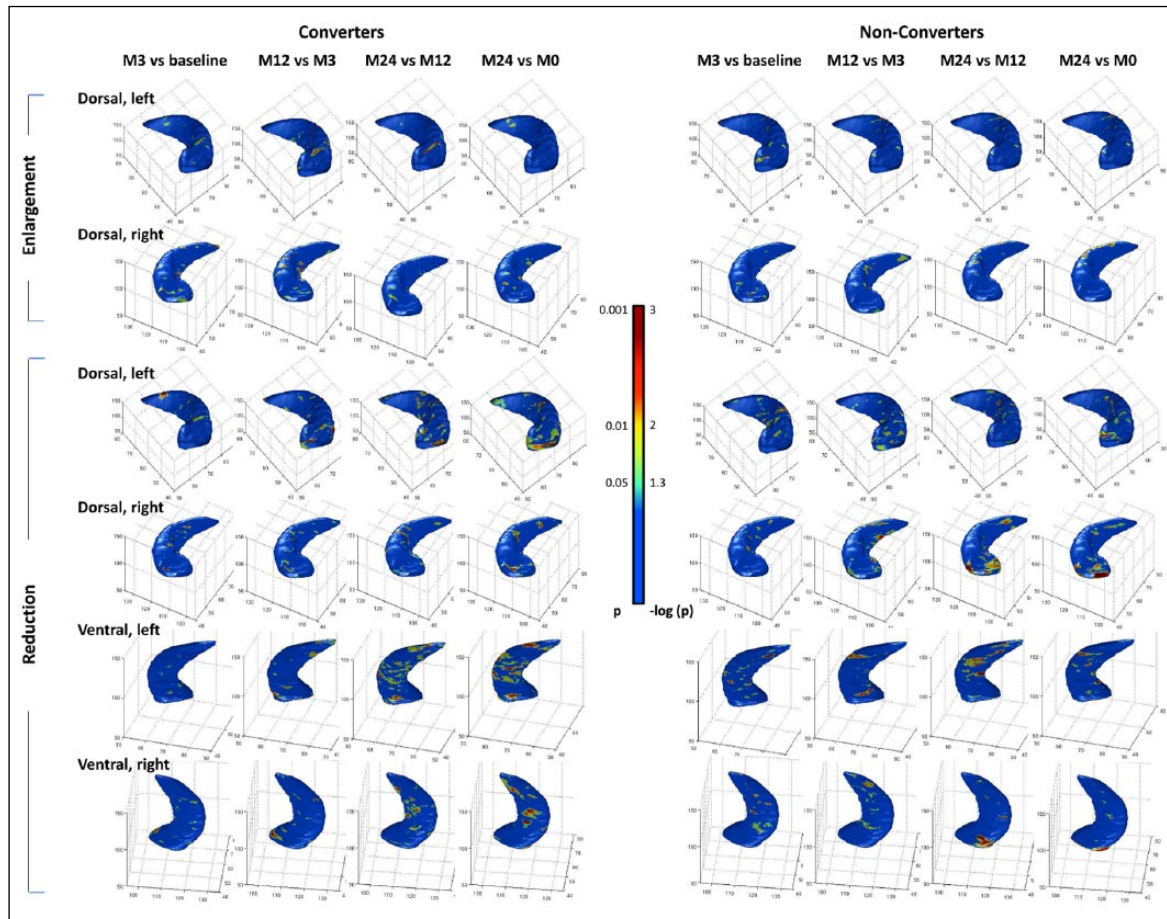


Figure 3. Hippocampal radial distance (RD) longitudinal modifications in clinically isolated syndrome converting to clinically defined MS (left side) versus non-converter patients (right side) with distinction between regions of significant RD enlargement and reduction; p value ranges in the color bar are reported as $-\log(p)$ value). M3: 3 months; M12: 12 months.

unexpectedly, given the relative cognitive preservation of our patients at this test, we found no correlation. We cannot rule out that the use of a more extensive cognitive assessment, with specific tests for hippocampal function, and a longer follow-up would have allowed defining whether such a DG enlargement confers a protection toward the development of cognitive deficits.

Our study has some limitations, including the small sample size, the relatively low field strength, the possible effect of sex on the hippocampal atrophy profile, and the lack of sequences specific for visualizing GM lesions (for instance, double inversion recovery). From a methodological point of view, we cannot exclude that changes at the boundaries (especially when anatomy is altered) could bias the position of the medial core (i.e. redistributing changes over symmetrical vertices) or an “early ending” of the tail segmentation could affect the correspondences of vertices. However, our data do not show a symmetric behavior over hippocampal vertices

or inexplicable instability of HC group. Moreover, the compensation for head size was obtained through a linear transformation to the MNI space of the whole head. The transformation resulted to be heavily weighted for the skull dimension and correlated with the SIENAX scaling factors. On this issue, the literature reports the importance of correcting for head size in an accurate way.³⁵ Although paired longitudinal variations are free from this confounding effect, this can potentially affect group analysis. In addition, although the original isotropic resolution was maintained, the registration to standard space introduced interpolation. Admittedly, an inaccuracy of hippocampal head segmentation (due to the contiguity with the amygdala) could contribute to explain the RD oscillations observed in this region. Although other shape-based analysis (based on changes from an average distribution of vertex position) can be used to explore hippocampal modifications, we think that RD, which is measured from an intrinsic reference, could better identify changes intrinsic to the structure.

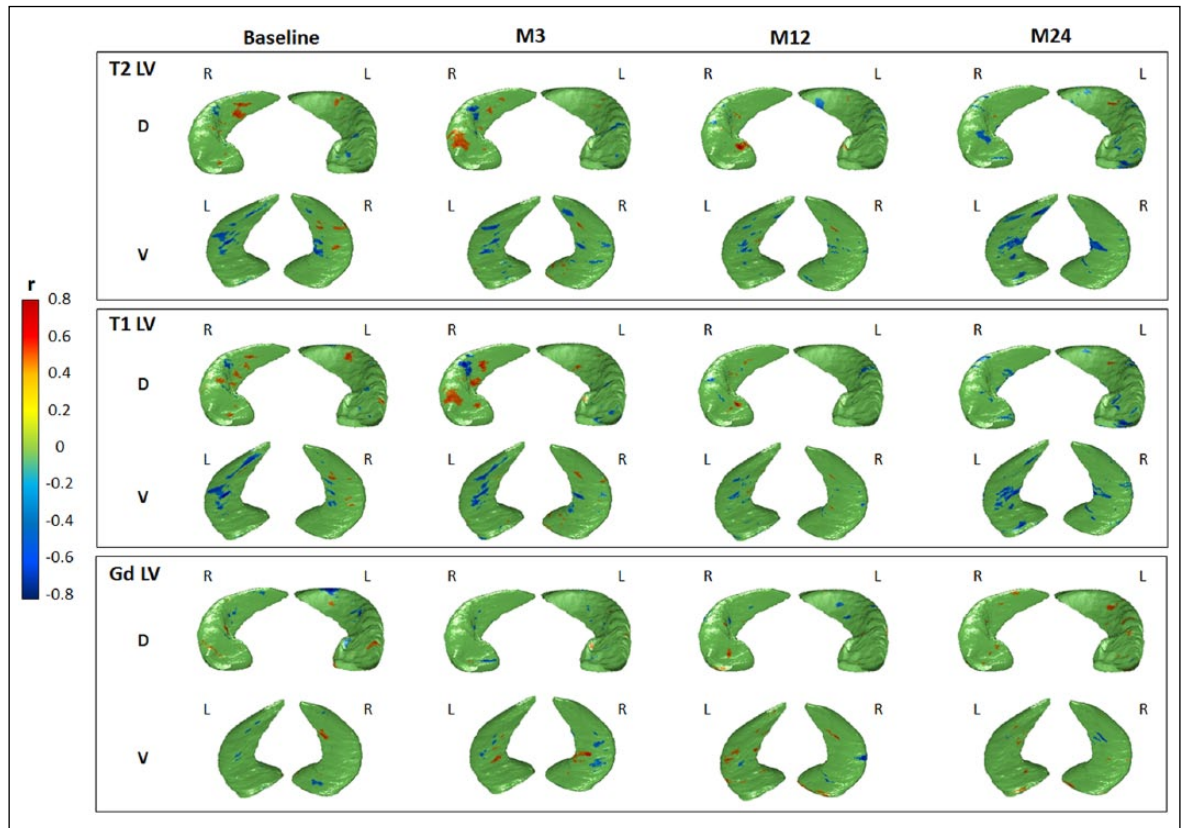


Figure 4. Correlation between radial distance (RD) and ipsilateral T2 lesion volume (LV), T1 LV, and gadolinium (Gd) LV at baseline, 3-, 12-, and 24-month follow-up. *R*-value ranges are shown in the color bars (only *R* values corresponding to $p < 0.05$ are shown). M3: 3 months; M12: 12 months; M24: 24 months; LV: lesion volume.

To conclude, despite an apparently preserved hippocampal volume, we observed local atrophy damage in CA1 and subiculum subfields, from the beginning of the disease, confirming the early presence of neurodegenerative mechanisms. Bilateral expansion of the DG subfield was also observed, which positively correlated with lesion burden and to conversion to MS, suggesting a possible response to focal WM damage. To better understand and confirm these findings, future studies should try to combine this type of analysis with a quantification of GM lesions and microstructural hippocampal alterations.

Declaration of Conflicting Interests

The author(s) declared the following potential conflicts of interest with respect to the research, authorship, and/or publication of this article: L.C., E.P., S.M., J.D., I.D.-B., J.D., and P.V. have nothing to disclose. M.A.R. received speakers' honoraria from Biogen Idec, Novartis, Genzyme, Sanofi-Aventis, Teva, Merck-Serono, and Roche, and receives research support from the Italian Ministry of Health

and Fondazione Italiana Sclerosi Multipla. M.F. is Editor-in-Chief of the *Journal of Neurology*; received compensation for consulting services and/or speaking activities from Biogen Idec, Merck-Serono, Novartis, Teva Pharmaceutical Industries; and receives research support from Biogen Idec, Merck-Serono, Novartis, Teva Pharmaceutical Industries, Roche, Italian Ministry of Health, Fondazione Italiana Sclerosi Multipla, and ARiSLA (Fondazione Italiana di Ricerca per la SLA).

Funding

The author(s) disclosed receipt of the following financial support for the research, authorship, and/or publication of this article: This study was partially supported by a grant from the Ministry of Science, Republic of Serbia (Project Number: 175031).

ORCID iDs

Massimo Filippi  <https://orcid.org/0000-0002-5485-0479>

Maria Assunta Rocca  <https://orcid.org/0000-0003-2358-4320>

References

1. Calabrese M, De Stefano N, Atzori M, et al. Detection of cortical inflammatory lesions by double inversion recovery magnetic resonance imaging in patients with multiple sclerosis. *Arch Neurol* 2007; 64: 1416–1422.
2. Geurts JJ and Barkhof F. Grey matter pathology in multiple sclerosis. *Lancet Neurol* 2008; 7: 841–851.
3. Roosendaal SD, Hulst HE, Vrenken H, et al. Structural and functional hippocampal changes in multiple sclerosis patients with intact memory function. *Radiology* 2010; 255: 595–604.
4. Sicotte NL, Kern KC, Giesser BS, et al. Regional hippocampal atrophy in multiple sclerosis. *Brain* 2008; 131: 1134–1141.
5. Longoni G, Rocca MA, Pagani E, et al. Deficits in memory and visuospatial learning correlate with regional hippocampal atrophy in MS. *Brain Struct Funct* 2015; 220: 435–444.
6. Geurts JJ, Bo L, Roosendaal SD, et al. Extensive hippocampal demyelination in multiple sclerosis. *J Neuropathol Exp Neurol* 2007; 66: 819–827.
7. Papadopoulos D, Dukes S, Patel R, et al. Substantial archaeocortical atrophy and neuronal loss in multiple sclerosis. *Brain Pathol* 2009; 19: 238–253.
8. Roosendaal SD, Moraal B, Vrenken H, et al. In vivo MR imaging of hippocampal lesions in multiple sclerosis. *J Magn Reson Imaging* 2008; 27: 726–731.
9. Woodhams PL, Celio MR, Ulfing N, et al. Morphological and functional correlates of borders in the entorhinal cortex and hippocampus. *Hippocampus* 1993; 3(S1): 303–311.
10. Aronica EM, Gorter JA, Grooms S, et al. Aurintricarboxylic acid prevents GLUR2 mRNA down-regulation and delayed neurodegeneration in hippocampal CA1 neurons of gerbil after global ischemia. *Proc Natl Acad Sci U S A* 1998; 95: 7115–7120.
11. Blumcke I, Pauli E, Clusmann H, et al. A new clinicopathological classification system for mesial temporal sclerosis. *Acta Neuropathol* 2007; 113: 235–244.
12. Spalding KL, Bergmann O, Alkass K, et al. Dynamics of hippocampal neurogenesis in adult humans. *Cell* 2013; 153: 1219–1227.
13. Clelland CD, Choi M, Romberg C, et al. A functional role for adult hippocampal neurogenesis in spatial pattern separation. *Science* 2009; 325: 210–213.
14. Lynch MA. Long-term potentiation and memory. *Physiol Rev* 2004; 84: 87–136.
15. Schmidt-Hieber C, Jonas P and Bischofberger J. Enhanced synaptic plasticity in newly generated granule cells of the adult hippocampus. *Nature* 2004; 429: 184–187.
16. Rocca MA, Longoni G, Pagani E, et al. In vivo evidence of hippocampal dentate gyrus expansion in multiple sclerosis. *Hum Brain Mapp* 2015; 36: 4702–4713.
17. Thompson PM, Hayashi KM, De Zubicaray GI, et al. Mapping hippocampal and ventricular change in Alzheimer disease. *Neuroimage* 2004; 22: 1754–1766.
18. Rocca MA, Preziosa P, Mesaros S, et al. Clinically isolated syndrome suggestive of multiple sclerosis: Dynamic patterns of gray and white matter changes—A 2-year MR imaging study. *Radiology* 2016; 278: 841–853.
19. Obradovic D, Petrovic M, Antanasijevic I, et al. The Brief Repeatable Battery: Psychometrics and normative values with age, education and gender corrections in a Serbian population. *Neurol Sci* 2012; 33: 1369–1374.
20. Portaccio E, Goretti B, Zipoli V, et al. Reliability, practice effects, and change indices for Rao’s Brief Repeatable Battery. *Mult Scler* 2010; 16: 611–617.
21. Polman CH, Reingold SC, Banwell B, et al. Diagnostic criteria for multiple sclerosis: 2010 revisions to the McDonald criteria. *Ann Neurol* 2011; 69: 292–302.
22. Studholme C, Hill DL and Hawkes DJ. Automated three-dimensional registration of magnetic resonance and positron emission tomography brain images by multiresolution optimization of voxel similarity measures. *Med Phys* 1997; 24: 25–35.
23. Pruessner JC, Li LM, Serles W, et al. Volumetry of hippocampus and amygdala with high-resolution MRI and three-dimensional analysis software: Minimizing the discrepancies between laboratories. *Cereb Cortex* 2000; 10: 433–442.
24. Iglesias JE, Van Leemput K, Augustinack J, et al. Bayesian longitudinal segmentation of hippocampal substructures in brain MRI using subject-specific atlases. *Neuroimage* 2016; 141: 542–555.
25. Santyr BG, Goubran M, Lau JC, et al. Investigation of hippocampal substructures in focal temporal lobe epilepsy with and without hippocampal sclerosis at 7T. *J Magn Reson Imaging* 2017; 45: 1359–1370.
26. Winner B, Kohl Z and Gage FH. Neurodegenerative disease and adult neurogenesis. *Eur J Neurosci* 2011; 33: 1139–1151.
27. Winner B and Winkler J. Adult neurogenesis in neurodegenerative diseases. *Cold Spring Harb Perspect Biol* 2015; 7: a021287.
28. Monje ML, Toda H and Palmer TD. Inflammatory blockade restores adult hippocampal neurogenesis. *Science* 2003; 302: 1760–1765.

29. Van Praag H, Schinder AF, Christie BR, et al. Functional neurogenesis in the adult hippocampus. *Nature* 2002; 415: 1030–1034.
30. Giannakopoulou A, Lyras GA and Grigoriadis N. Long-term effects of autoimmune CNS inflammation on adult hippocampal neurogenesis. *J Neurosci Res* 2017; 95: 1446–1458.
31. Luo C, Ikegaya Y and Koyama R. Microglia and neurogenesis in the epileptic dentate gyrus. *Neurogenesis* 2016; 3: e1235525.
32. Giannetti P, Politis M, Su P, et al. Increased PK11195-PET binding in normal-appearing white matter in clinically isolated syndrome. *Brain* 2015; 138: 110–119.
33. Sun Y, Hong F, Zhang L, et al. The sphingosine-1-phosphate analogue, FTY-720, promotes the proliferation of embryonic neural stem cells, enhances hippocampal neurogenesis and learning and memory abilities in adult mice. *Br J Pharmacol* 2016; 173: 2793–2807.
34. Giannakopoulou A, Grigoriadis N, Bekiari C, et al. Acute inflammation alters adult hippocampal neurogenesis in a multiple sclerosis mouse model. *J Neurosci Res* 2013; 91: 890–900.
35. Nordenskjold R, Malmberg F, Larsson EM, et al. Intracranial volume estimated with commonly used methods could introduce bias in studies including brain volume measurements. *Neuroimage* 2013; 83: 355–360.

Visit SAGE journals online
[journals.sagepub.com/
home/msj](http://journals.sagepub.com/home/msj)

 SAGE journals